

The MEXSAS2 Sample and the Ensemble X-ray Variability of Quasars

R. Serafinelli^{1,2,*}, F. Vagnetti¹, E. Chiaraluce^{1,2}, and R. Middei³

¹*Dipartimento di Fisica, Università di Roma Tor Vergata, Roma, Italy*

²*Dipartimento di Fisica, Università di Roma Sapienza, Roma, Italy*

³*Dipartimento di Matematica e Fisica, Università Roma Tre, Roma, Italy*

Correspondence*:

Roberto Serafinelli

roberto.serafinelli@roma2.infn.it

ABSTRACT

We present the second Multi-Epoch X-ray Serendipitous AGN Sample (MEXSAS2), extracted from the 6th release of the XMM Serendipitous Source Catalogue (XMMSSC-DR6), cross-matched with Sloan Digital Sky Survey quasar catalogues DR7Q and DR12Q. Our sample also includes the available measurements for masses, bolometric luminosities, and Eddington ratios. Analyses of the ensemble structure function and spectral variability are presented, together with their dependences on such parameters. We confirm a decrease of the structure function with the X-ray luminosity, and find a weak dependence on the black hole mass. We introduce a new spectral variability estimator, taking errors on both fluxes and spectral indices into account. We confirm an ensemble softer when brighter trend, with no dependence of such estimator on black hole mass, Eddington ratio, redshift, X-ray and bolometric luminosity.

Keywords: Catalogs - Quasars - Spectral Variability - Structure Function - X-rays

1 THE MEXSAS2 CATALOGUE

We present here the MEXSAS2 catalogue, obtained from the sixth release of the XMM Newton Serendipitous Source Catalogue (XMMSSC-DR6, Rosen et al., 2016), combined with both SDSS-DR7Q (Schneider et al., 2010) and SDSS-DR12Q quasar catalogues (Pâris et al., 2017). The MEXSAS2 catalogue is the updated version of MEXSAS (Multi-Epoch XMM Serendipitous AGN Sample), published by Vagnetti et al. (2016). It contains 9735 X-ray observations for 3366 quasars, which increases by about 25% the numbers of the previous version (7837 observations, 2700 quasars). It only contains sources with more than one observation, and it is therefore ideal for variability studies.

We complement the catalogue with measurements of black hole masses, bolometric luminosities and Eddington ratios, which are available for 3138 quasars (93%) from the catalogues by Shen et al. (2011) for the sources listed in SDSS-DR7Q, and by Kozłowski (2017) for SDSS-DR12Q. We use homogeneous criteria to derive the masses and bolometric luminosities from the two catalogues, adapting their criteria, which are slightly different for the redshift intervals where two different broad lines and two continuum luminosities are available. In fact, Shen et al. (2011) adopts different single-epoch virial estimates sharply dividing at redshift $z = 0.7$ for choosing between $H\beta$ and $MgII(2798\text{\AA})$ relations, and at $z = 1.9$ for $Mg II(2798\text{\AA})$ and $CIV(1549\text{\AA})$. A similar option is adopted for computing bolometric luminosities from the continua at 5100\AA or 3000\AA dividing at $z = 0.7$, and at 3000\AA or 1350\AA dividing at $z = 1.9$. The

criteria adopted by Kozłowski (2017) are instead to prefer the Mg II black hole mass estimate when available, rather than that from C IV, which is biased from various effects, and to compute bolometric luminosity as a weighted average of those derived from two different available continua. However, Kozłowski (2017) also find that the DR7Q line widths (which are derived from detailed fits of spectral components) are generally more reliable than the DR12Q ones (which are derived from principal component analysis), thus they are to be preferred, when available. To apply the same criteria to the mass and luminosity data from both DR7Q and DR12Q, we adopt the following choice: (i) for quasars included only in DR12Q and not in DR7Q, we take the estimates by Kozłowski (2017) (2178 objects); (ii) for quasars included in both catalogues or only in DR7Q, and in redshift intervals with only one broad line and one continuum luminosity available ($z \lesssim 0.35$, $0.9 \lesssim z \lesssim 1.5$, $z \gtrsim 2.25$), we take the estimates by Shen et al. (2011) (442 objects); (iii) for quasars included in both catalogues or only in DR7Q, in redshift intervals with two broad lines and continua ($0.35 \lesssim z \lesssim 0.9$, $1.5 \lesssim z \lesssim 2.25$), we apply the Kozłowski (2017) criteria to the DR7Q data, deriving new estimates (518 objects).

The catalogue, including X-ray measurements from XMMSSC and quasar data from SDSS and from our elaboration, will be published elsewhere (Vagnetti et al, in preparation). Here we provide preliminary results of our ensemble analyses of the X-ray variability.

2 FLUX VARIABILITY AND STRUCTURE FUNCTION

We compute the structure function according to Vagnetti et al. (2016), as a r.m.s. difference of the X-ray flux measured at two epochs differing by τ in the rest-frame, and corrected for the noise contribution,

$$SF(\tau) \equiv \sqrt{\langle [\log f_X(t + \tau) - \log f_X(t)]^2 \rangle - \sigma_{noise, SF}^2} \quad , \quad (1)$$

where $\sigma_{noise, SF}^2 = \langle \sigma_n^2(t) + \sigma_n^2(t + \tau) \rangle$ is the quadratic contribution of the photometric noise to the observed variations, σ_n being the error on $\log f_X$ at each given time.

We use mainly EPIC X-ray fluxes in the XMM-Newton band 9 (0.5-4.5 KeV), as in our previous papers (Vagnetti et al., 2011, 2016).

The SF can be fitted by a power-law $SF \propto \tau^b$. For the whole sample we find a slope $b = 0.11 \pm 0.01$. The SFs in bins of X-ray luminosity and black hole mass are shown in Fig. 1. We confirm a strong anti-correlation with X-ray luminosity, approximately as $L_X^{-0.22}$, with correlation coefficient $r = -0.92$ and null probability $p(> r) = 0.04$, and no dependence on redshift, similarly to Vagnetti et al. (2016). There is an apparent decrease of the SF with black hole mass, approximately as $M_{BH}^{-0.15}$, with $r = -0.97$ and $p(> r) = 0.03$, but partial correlation analysis suggests that this is due to the strong correlation of mass with X-ray luminosity. Limiting the analysis to the luminosity interval $10^{44} \text{ erg/s} < L_X < 10^{45} \text{ erg/s}$, the mass-luminosity correlation reduces ($r = -0.83$, $p(> r) = 0.06$), and the dependence of the SF on black hole mass is weaker, $\propto M_{BH}^{-0.06}$. We find neither dependence on bolometric luminosity nor on Eddington ratio.

3 SPECTRAL VARIABILITY

We update the analysis of the spectral variability parameter, initially introduced by Trevese and Vagnetti (2002) and recently adapted to the X-ray band by Serafinelli et al. (2017)

$$\beta = -\frac{\Delta\Gamma}{\Delta \log f_X} \quad , \quad (2)$$

relating variations of the photon index Γ with those of the X-ray flux in a given band.

The spectra of most Seyfert galaxies with Eddington ratios above 0.01 typically become steeper in their brighter phases (e.g. Markowitz et al., 2003; Sobolewska and Papadakis, 2009; Connolly et al., 2016), as well as for many galactic black hole binary systems (e.g. Remillard and McClintock, 2006; Done et al., 2007; Dong et al., 2014). This is known as ‘softer when brighter’ behaviour and translates to a negative β value according to Eq. 2. We also found this ‘softer when brighter’ behaviour, obtaining $\beta = -0.69 \pm 0.03$ in our ensemble analysis, for the previous version of the MEXSAS sample, using fluxes in the soft X-ray band 0.5-2 keV, and computing variations with respect to the mean values of each source (Serafinelli et al., 2017).

Since the ensemble correlation between $\Delta\Gamma$ and $\Delta \log f_X$ contains a large scatter, also due to the large measurement errors for the fainter sources, we fit a linear relation $\Delta\Gamma \propto \Delta \log f_X$ to the MEXSAS2 data set taking the uncertainties in both variables into account. We run a high number of linear fits replacing original data with Gaussian distributed values within the associated error box. Moreover, following Isobe et al. (1990), we computed both ordinary least squares regressions $OLS(Y|X)$ of the dependent variable Y on the independent variable X (which result we call for brevity β_{xy}), the inverse regression $OLS(X|Y)$ (β_{yx}), and the bisector:

$$\beta_{bis} = \frac{\beta_{xy}\beta_{yx} - 1 + \sqrt{(1 + \beta_{xy}^2)(1 + \beta_{yx}^2)}}{\beta_{xy} + \beta_{yx}} \quad (3)$$

For the whole sample, we find ensemble values $\beta_{xy} = -0.22 \pm 0.04$ and $\beta_{bis} = -1.22 \pm 0.05$, confirming the ‘softer when brighter’ behaviour for both spectral variability parameters (see Fig. 2).

We then divide our sample in bins of soft X-ray flux, to show that the resulting β does not change within the errors (see Fig. 3). In fact this was expected, because measurement errors do affect the estimate of β , but this must reflect an intrinsic relation between the flux and slope variations which should not change with an observational parameter like the average flux of the sources.

We also divide our sample in bins of black hole mass, M_{BH} , and show the result in Fig. 3. Both β_{xy} and β_{bis} are independent of M_{BH} within the errors, and always compatible with their overall ensemble values. We similarly analyse possible dependencies on Eddington ratio, redshift, X-ray and bolometric luminosities, finding no evidence of change. This analysis will be reported in an upcoming paper (Vagnetti et al., in prep.).

4 SUMMARY

- We have updated our X-ray quasar catalogue MEXSAS to MEXSAS2.
- We have confirmed our previous results for the structure function dependence on X-ray luminosity, and no dependence on redshift; we find a weak dependence on black hole mass, and no dependence on bolometric luminosity and Eddington ratio.
- We have developed new spectral variability estimators, by computing ordinary least squares and bisector fits with errors in both variables.
- We obtain ‘softer when brighter’ trends for the new MEXSAS2 sample using both estimators.
- Our spectral variability estimates, that also take errors on both fluxes and spectral indices into account, do not present a dependence on the flux.
- No trend with black hole mass, Eddington ratio, redshift, X-ray and bolometric luminosities is found, in agreement with our previous results (Serafinelli et al., 2017).

AUTHOR CONTRIBUTIONS

RS performed the spectral variability analysis and wrote part of the text, FV was responsible for the idea that resulted in the paper and also contributed to the text, EC built the dataset of the MEXSAS2 catalogue, RM performed the structure function analysis.

REFERENCES

- Connolly, S. D., McHardy, I. M., Skipper, C. J., and Emmanoulopoulos, D. (2016). Long-term X-ray spectral variability in AGN from the Palomar sample observed by Swift. *MNRAS* 459, 3963–3985. doi:10.1093/mnras/stw878
- Done, C., Gierliński, M., and Kubota, A. (2007). Modelling the behaviour of accretion flows in X-ray binaries. Everything you always wanted to know about accretion but were afraid to ask. *A&A Rev.* 15, 1–66. doi:10.1007/s00159-007-0006-1
- Dong, A.-J., Wu, Q., and Cao, X.-F. (2014). A New Fundamental Plane for Radiatively Efficient Black-hole Sources. *ApJ* 787, L20. doi:10.1088/2041-8205/787/2/L20
- Isobe, T., Feigelson, E. D., Akritas, M. G., and Babu, G. J. (1990). Linear regression in astronomy. *ApJ* 364, 104–113. doi:10.1086/169390
- Kozłowski, S. (2017). Virial Black Hole Mass Estimates for 280,000 AGNs from the SDSS Broadband Photometry and Single-epoch Spectra. *ApJS* 228, 9. doi:10.3847/1538-4365/228/1/9
- Markowitz, A., Edelson, R., and Vaughan, S. (2003). Long-Term X-Ray Spectral Variability in Seyfert 1 Galaxies. *ApJ* 598, 935–955. doi:10.1086/379103
- Pâris, I., Petitjean, P., Ross, N. P., Myers, A. D., Aubourg, É., Streblyanska, A., et al. (2017). The Sloan Digital Sky Survey Quasar Catalog: Twelfth data release. *A&A* 597, A79. doi:10.1051/0004-6361/201527999
- Remillard, R. A. and McClintock, J. E. (2006). X-Ray Properties of Black-Hole Binaries. *ARA&A* 44, 49–92. doi:10.1146/annurev.astro.44.051905.092532
- Rosen, S. R., Webb, N. A., Watson, M. G., Ballet, J., Barret, D., Braito, V., et al. (2016). The XMM-Newton serendipitous survey. VII. The third XMM-Newton serendipitous source catalogue. *A&A* 590, A1. doi:10.1051/0004-6361/201526416
- Schneider, D. P., Richards, G. T., Hall, P. B., Strauss, M. A., Anderson, S. F., Boroson, T. A., et al. (2010). The Sloan Digital Sky Survey Quasar Catalog. V. Seventh Data Release. *AJ* 139, 2360–2373. doi:10.1088/0004-6256/139/6/2360
- Serafinelli, R., Vagnetti, F., and Middei, R. (2017). Quasar spectral variability from the XMM-Newton serendipitous source catalogue. *A&A* 600, A101. doi:10.1051/0004-6361/201629885
- Shen, Y., Richards, G. T., Strauss, M. A., Hall, P. B., Schneider, D. P., Snedden, S., et al. (2011). A Catalog of Quasar Properties from Sloan Digital Sky Survey Data Release 7. *ApJS* 194, 45. doi:10.1088/0067-0049/194/2/45
- Sobolewska, M. A. and Papadakis, I. E. (2009). The long-term X-ray spectral variability of AGN. *MNRAS* 399, 1597–1610. doi:10.1111/j.1365-2966.2009.15382.x
- Trevese, D. and Vagnetti, F. (2002). Quasar Spectral Slope Variability in the Optical Band. *ApJ* 564, 624–630. doi:10.1086/324541
- Vagnetti, F., Middei, R., Antonucci, M., Paolillo, M., and Serafinelli, R. (2016). Ensemble X-ray variability of active galactic nuclei. II. Excess variance and updated structure function. *A&A* 593, A55. doi:10.1051/0004-6361/201629057

Vagnetti, F., Turriziani, S., and Trevese, D. (2011). Ensemble X-ray variability of active galactic nuclei from serendipitous source catalogues. *A&A* 536, A84. doi:10.1051/0004-6361/201118072

FIGURE CAPTIONS

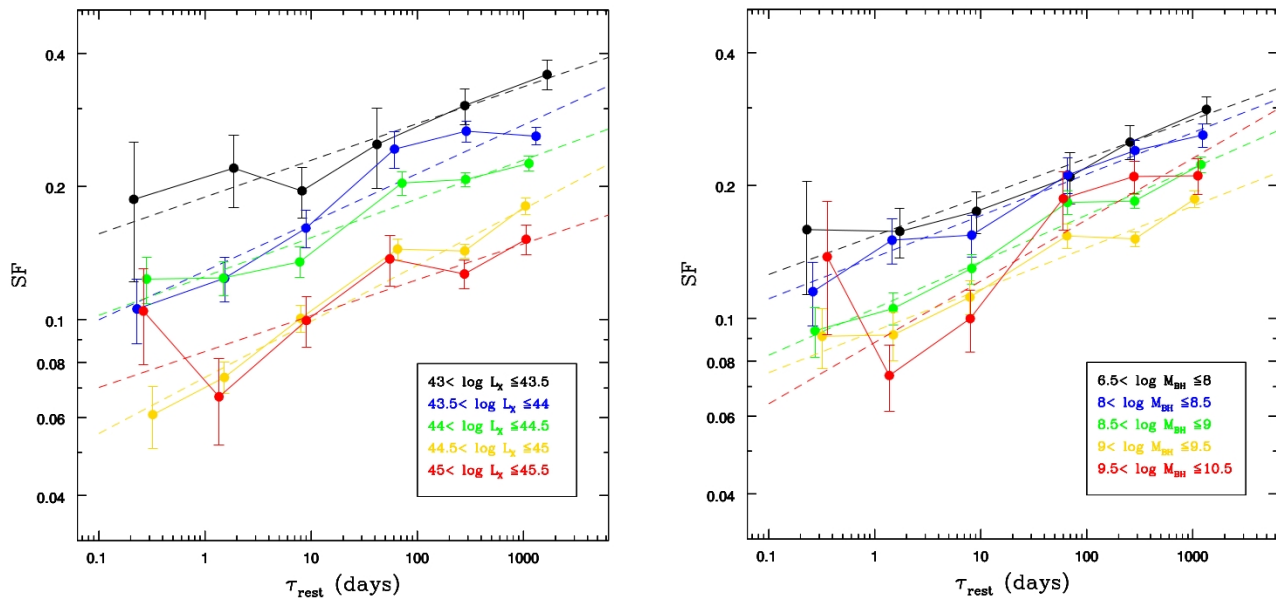


Figure 1. The structure function in bins of X-ray luminosity L_X and black hole mass M_{BH} (data and continuous lines) with power-law fits (dashed lines). *Left panel:* Black, $43 < \log L_X \leq 43.5$; blue, $43.5 < \log L_X \leq 44$; green, $44 < \log L_X \leq 44.5$; yellow, $44.5 < \log L_X \leq 45$; red, $45 < \log L_X \leq 45.5$. *Right panel:* Black, $6.5 < \log M_{BH} \leq 8$; blue, $8 < \log M_{BH} \leq 8.5$; green, $8.5 < \log M_{BH} \leq 9$; yellow, $9 < \log M_{BH} \leq 9.5$; red, $9.5 < \log M_{BH} \leq 10.5$.

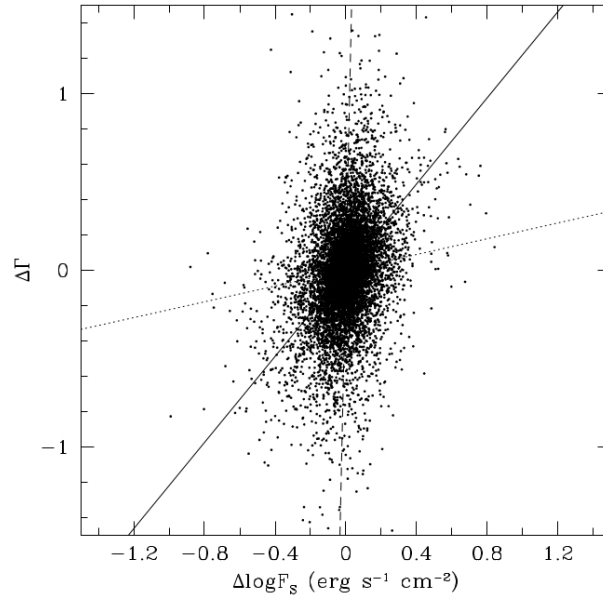


Figure 2. The ensemble correlation between the variations of the photon index $\Delta\Gamma$ and the variations of the logarithmic flux $\Delta\log F$ are shown. The dotted line represents β_{xy} , the dashed line represents β_{yx} , while the bisector β_{bis} is shown as a continuous line.

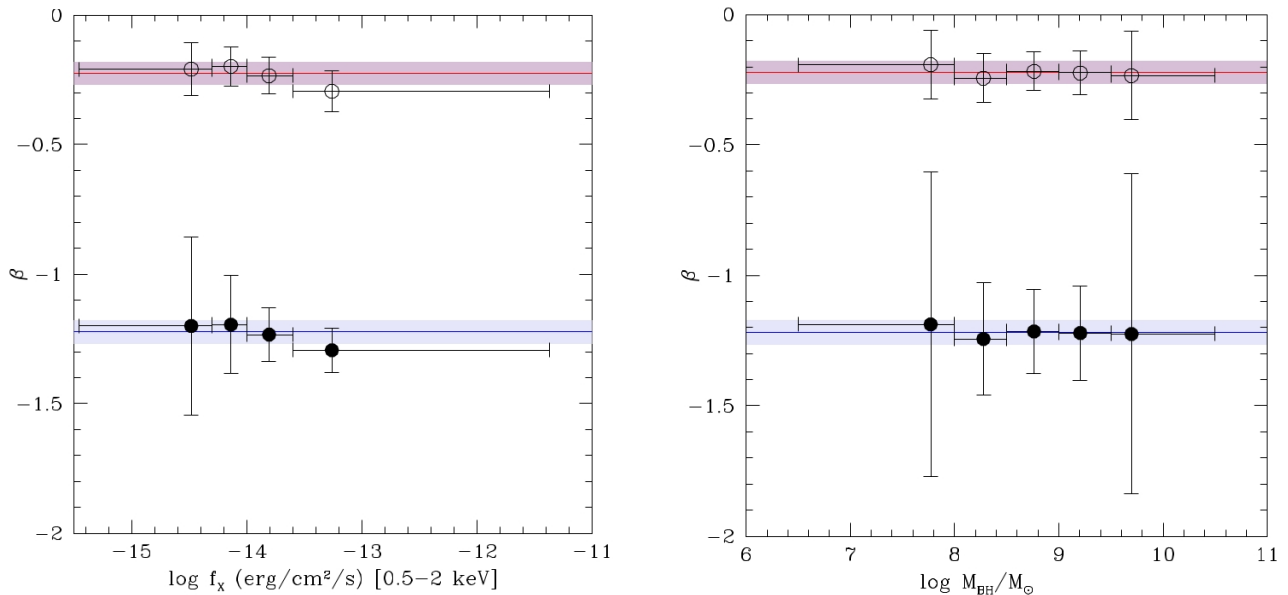


Figure 3. The dependence of β_{xy} and β_{bis} in bins of soft X-ray flux (*left panel*) and black hole mass (*right panel*). No dependence is found, and all the values of β_{xy} (empty circles) and β_{bis} (filled circles) are compatible with the corresponding ensemble values $\beta_{xy} = -0.22 \pm 0.04$ and $\beta_{bis} = -1.22 \pm 0.05$, which are indicated respectively by the red and blue lines, and by the lighter bands for the uncertainties. The horizontal bars indicate bin widths, not errors.